Biogeosciences, 11, 6539–6552, 2014
www.biogeosciences.net/11/6539/2014/
doi:10.5194/bg-11-6539-2014

Biogeosciences Open Access

Effect of ablation rings and soil temperature on 3-year spring CO_2 efflux along the Dalton Highway, Alaska

Y. Kim

International Arctic Research Center, University of Alaska Fairbanks, Fairbanks, AK 99775-7335, USA

Correspondence to: Y. Kim (kimyw@iarc.uaf.edu)

Received: 22 November 2013 – Published in Biogeosciences Discuss.: 6 March 2014
Revised: 18 September 2014 – Accepted: 9 October 2014 – Published: 1 December 2014

Abstract. Winter and spring soil CO_2 efflux measurements represent a significant component in the assessment of annual carbon budgets of tundra and boreal forest ecosystems, reflecting responses to climate change in the Arctic. This study was conducted in order to quantify CO_2 efflux, using a portable chamber system at representative sites along the Dalton Highway. Study sites included three tundra, two white spruce, and three black spruce forest locations during the winter and spring seasons of 2010–2012; the study of these sites promised better understanding of winter and spring carbon contributions to the annual carbon budget, as well as the respective ablation-ring effects during spring. Three-year spring CO_2 efflux depends on soil temperature at 5 cm depth on a regional scale. At their highest, Q_{10} values were 4.2×10^6, within the exposed tussock tundra of the upland tundra site, which tundra soils warmed from −0.9 to 0.5 °C, involving soil microbial activity. From the forest census (400 m^2) of the two white spruce forest sites, CO_2 emissions were estimated as 0.09–0.36 $gC\,m^{-2}\,day^{-1}$ in winter and 0.14–4.95 $gC\,m^{-2}\,day^{-1}$ in spring, corresponding to 1–3 % and 1–27 % of annual carbon, respectively. Contributions from spring CO_2 emissions are likely to increase as exposed soils widen in average length (major axis) from the east-, west-, south-, and north-side lengths (minor axis). Considering the periods of winter and spring seasons across tundra and boreal forests, average winter- and spring-seasonal CO_2 contributions to annual carbon budgets correspond roughly to 14–22 % for tundra and 9–24 % for boreal forest sites during 2011 and 2012. Spring carbon contributions, such as growing season CO_2 emissions, are sensitive to subtle changes at the onset of spring and during the snow-covered period in northern high latitudes, in response to recent Arctic climate change.

1 Introduction

Northern high latitudes exhibit Arctic climate change quite prominently through increasing air temperature, deepening active layers, thawing permafrost, changing snow cover, increasing shrub abundance, greening in tundra and browning in boreal forest ecosystems, and a prolonged vegetation growing season within terrestrial ecosystems (Sturm et al., 2001; ACIA, 2005; Verbyla, 2008; AMAP, 2011; de Jong et al., 2011; Bhatt et al., 2013). Terrestrial ecosystem carbon (e.g., CO_2 and CH_4) is obviously susceptible to these climate change responses (Chapin et al., 2000). Of these, it is no exaggeration to say that temperature is a significant driver for positive feedbacks on regional and pan-Arctic scales (Chapin et al., 2000; ACIA, 2004). Carbon dynamics in tundra and boreal forest ecosystems display temperature dependence – the so-called Q_{10} value – based on many field-based and modeling observations (Xu and Qi, 2001; Davidson and Jassens, 2006; Bond-Lamberty and Thomson, 2010; Mahecha et al., 2010). Bond-Lamberty and Thomson (2010) evaluated global soil respiration at 98 ± 12 GtC (1 GtC $= 10^{15}$ gC), showing an increase of 0.1 GtC $year^{-1}$ over 2 decades. This suggests a CO_2 emission response factor of 1.5 compared to air temperature (Q_{10}), consistent with an enhanced response from the terrestrial carbon cycle to global climate change (Bond-Lamberty and Thomson, 2010).

Soil CO_2 efflux, produced by the decomposition of soil organic carbon and roots, signifies the second largest terrestrial carbon source on both time and space scales (Raich and Schlesinger, 1992; Schlesinger and Andrews, 2000). Recently, the magnitude of soil CO_2 efflux has seemed to depend on tundra greening and boreal forest browning (Verbyla, 2008; Bhatt et al., 2010; Parent and Verbyla, 2010), as well as on the timing of both snow disappearance and

the snow-covered period (Stone et al., 2002; McDonald et al., 2004; Sturm et al., 2005). During the seasonally snow-covered period, winter CO_2 efflux measurements have heretofore been gathered in tundra (Oechel et al., 1997; Fahnestock et al., 1998, 1998; Björkman et al., 2010; Kim et al., 2013), alpine and subalpine forests (Brooks et al., 1996; Mast et al., 1998; Monson et al., 2006a, b), and boreal forests (Hardy et al., 1995; Winston et al., 1995, 1997; Kim et al., 2007, 2013), accounting for 10–30 % of the variability in annual carbon emissions. However, it is difficult to determine the timing of snow disappearance in the early spring season, due to shorter snow disappearance time spans, including changes of $-0.13\,\mathrm{day\,year^{-1}}$ over 60 years in Barrow, Alaska, according to NOAA/CMDL historical data (Stone et al., 2002), and $-0.94\,\mathrm{day\,year^{-1}}$ over 14 years according to microwave remote sensing (McDonald et al., 2004). Such shifts may cause decreased Arctic winter CO_2 efflux, as well as increased efflux during the vegetation growth period (Sturm et al., 2005), resulting from changes in solar radiation (e.g., energy exchange) (Eugster et al., 2000). It is important, therefore, to understand and qualify soil carbon balance – whether it shows the acceleration of photosynthesis and respiration or their decline – as it controls the terrestrial carbon budget in response to a changing climate in northern high latitudes.

Indeed, soil temperature and moisture are important parameters in regulating soil CO_2 efflux across tundra and boreal forest ecosystems (Lloyd and Taylor, 1994; Davidson et al., 1998; Xu and Qi, 2001; Davidson and Janssens, 2006; Rayment and Jarvis, 2000; Kim et al., 2007, 2013), and these parameters must be validated for terrestrial ecosystem process-based models, for the assessment of carbon budgets on regional and global scales. Also noted here are snow depth and snow crust, which slightly affect winter/spring CO_2 efflux in vegetation types across the North Slope of Alaska ($R^2 = 0.19$; Fahnestock et al., 1998), and in subalpine soils of Rocky Mountain National Park, Colorado (Mast et al., 1998), respectively. Further work is needed to evaluate these environmental parameters, which influence soil CO_2 efflux during seasonally snow-covered and snow-free periods, across both tundra and boreal forest ecosystems.

The aims of this study are to (1) determine the environmental parameters resolving CO_2 efflux in exposed and snow-covered soils along the Dalton Highway; (2) understand the characteristics of CO_2 efflux in exposed and snow-covered soils, considering the effect of ablation rings during the spring season; and (3) assess the contributions from winter and spring carbon toward the annual carbon balance during the winter and spring seasons of 2010–2012, based on a constant area ($400\,\mathrm{m^2}$) within white spruce sites during winter and spring periods.

2 Materials and methods

2.1 Sampling descriptions and methods

Using a dynamic chamber system method, soil CO_2 efflux was measured at three tundra sites and five boreal forest sites along the Dalton Highway, over a distance of 660 km, during the winter and spring seasons of 2010–2012, as shown in Fig. 1. Site information is shown in Table 1; sites were located within coastal tundra (CT, northernmost), upland tundra (UT, between CT and SaT), subalpine tundra (SaT, north slope of Brooks Range), ecotone (TZ, a transition zone between tundra and boreal forest), a white spruce forest in Gold Creek (GC), a younger black spruce forest near Coldfoot (BC), and two black spruce forest sites along the upper and lower Yukon River (YU and YL, southernmost). Periods of flux measurement were 12–25 January 2010, 26 February–12 March 2011, and 5–22 March 2012 for winter; and 7–23 April 2010, 23 April–4 May 2011, and 21 April–3 May 2012 for spring.

Sites were classified as three ecotypes: tundra (CT, UT, and SaT), white spruce forest (TZ and GC), and black spruce forest (BC, YU, and YL), depending on dominant vegetation and permafrost. Dominant species are listed in Table 1. The general distribution of Alaska tundra vegetation amounts to moss, sedge, and dwarf shrubs (Bliss and Matveyeva, 1992). Patterns in the northern foothills of the North Slope include cotton-grass tussock tundra, bryophyte, lichen, and graminoid communities (Raynolds et al., 2006). Meanwhile, the boreal forest extends across the lowlands and uplands of the Tanana–Yukon flats, comprising white and black spruce and deciduous forests (Raynolds et al., 2006; Kim et al., 2013). Continuous and discontinuous permafrost underlies the tundra and boreal forest ecosystems, respectively, while no permafrost exists throughout the white spruce forest. It is difficult to represent average snow depth at each site due to different measuring periods for the winter season, though spring snow depth is listed in Table 2. The measuring periods for air temperature during winter and spring were defined as 1 November–31 March and 15 April–15 June, respectively. Table 2 shows the average, standard deviation (SD), minimum, and maximum for air temperature, measured at 1.3 m above the soil surface during the winter and spring seasons of 2010–2012. In order to evaluate the existence of snow crust as it affects CO_2 emissions through the snowpack to the atmosphere, CO_2 efflux measurements were conducted before and after the removal of snow crust at each site.

Seasonally covered snowpack began to melt in areas surrounding boreal forest trees and at the top of tundra tussock during spring, as shown in Fig. 2. The spring snow-melting mechanism around trees proceeds as follows (Kojima, 2001): (1) tree trunks directly absorb strong solar energy (e.g., short wavelength) from the sun, due to smaller reflectance from trees than from the snow surface; (2) temperatures of tree

Table 1. Site information for black spruce, white spruce, and tundra sites across the haul road of Alaska during the winter and spring seasons of 2010–2012.

Ecosystem	Site	Latitude (N)	Longitude (W)	Elevation (m a.s.l.)	Aspect	Slope (°)	Dominant species
Black spruce	YL	65°50′30.5″	149°38′44.2″	360	N65E	6	*Picea mariana, Ledum palustre, Vaccinium vitis-idaea, Vaccinium uliginosum*
	YU	66°04′48.2″	150°09′56.3″	220	N50W	5	*Picea mariana, Vaccinium vitis-idaea, Vaccinium uliginosum, Betula glandulosa*
	BC	67°10′47.6″	150°18′24.9″	349	N60W	5	*Picea mariana, Vaccinium vitis-idaea, Ledum palustre, Betula glandulosa*
White spruce	GC	67°44′09.5″	149°45′23.1″	478	N55W	2	*Picea glauca, Betula glandulosa, Vaccinium uliginosum, Vaccinium vitis-idaea*
	TZ	67°59′27.5″	149°45′37.5″	690	N80W	10	*Picea glauca, Vaccinium uliginosum, Vaccinium vitis-idaea, Empetrum nigrum*
Tundra	SaT	68°10′32.4″	149°26′26.3″	1064	N60E	5	*Vaccinium uliginosum, Dryas integrifolia, Carex bigelowii, Salix reticulata*
	UT	68°53′57.7″	148°52′02.5″	425	S60E	3	*Eriophorum vaginatum, Ledum palustre, Betula glandulosa, Vaccinium vitis-idaea*
	CT	69°50′26.8″	148°42′31.6″	35	S40W	2	*Eriophorum vaginatum, Betula glandulosa, Salix pulchra, Carex lugens*

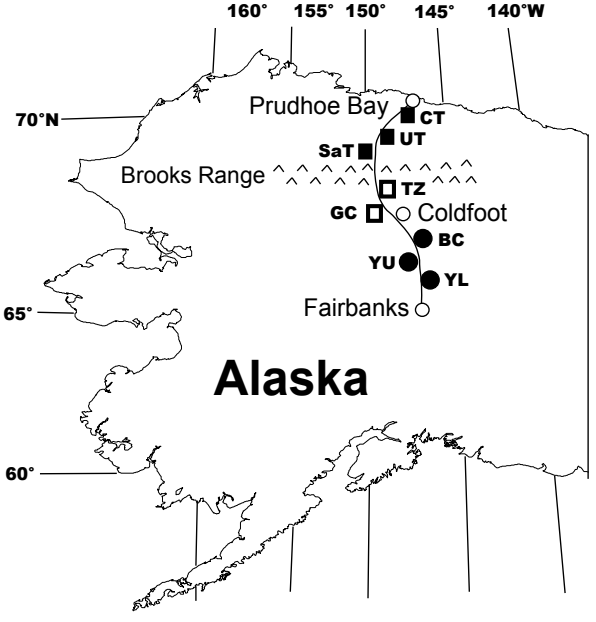

Figure 1. Site locations along the Dalton Highway of Alaska, during the winter and spring seasons of 2010–2012. Solid circles are black spruce forest sites, open squares are white spruce forest sites, and solid squares denote tundra sites.

stems themselves increase; (3) warmed stems emit radiation as long wavelengths during nighttime; (4) snow surrounding tree trunks melts in concentric circles (e.g., ablation rings) around stems (Winston et al., 1995, 1997); (5) dents surrounding stems and tussock open in round and oval shapes; (6) dents extend to the ground; (7) soil around stems issues a face; (8) ground is exposed as the temperature rises; and finally (9) larger dents from melting snow are completed down to the bases of stems, as shown in Fig. 2. For the Canadian boreal forest, Winston et al. (1995, 1997) explained that an important mechanism of CO_2 transport through the forest snowpack was by macrochannels along trunks and stems, as previously described regarding snow-melting mechanisms near the tree stem. Soil CO_2 efflux was measured in the exposed and snow-covered soils of boreal forests (Fig. 2a–c) and tussock tundra (Fig. 2d) during spring. At boreal forest sites, efflux measurements were conducted in exposed and snow-covered soils in four directions from the stems of the white spruce forest, at intervals of 50–60 cm from the stem, due to differences in snowmelt rate from four directions of solar radiation. Generally, the expansion of exposed soil on the south side is much faster and wider than on other sides, as shown in Fig. 2b.

Taking into account the contribution from spring CO_2 efflux by the effect of ablation rings in the white spruce forest, the forest census was investigated at the TZ and GC sites. Tree density and height within a 20 m × 20 m plot were 32 trees/400 m^2 and 5.1 m at TZ, and 30 trees/400 m^2 and 8.8 m at GC, respectively (Suzuki et al., 2013). I assumed here that the extent of the lowest branch of the targeted white spruce is the same as in the exposed area, due to the relatively lower snowpack under branches of white spruce compared

Table 2. Snow depth during the spring season of 14 April–14 June and air temperatures during the winter seasons of November–March of 2011 and 2012.

Year	Site	Snow depth (cm)	Air temperature in winter (°C)				Air temperature in spring (°C)			
			Average	SD	Min	Max	Average	SD	Min	Max
2010	CT	25	−22.0	9.0	−41.3	−2.0	−3.4	6.4	−14.2	12.5
	UT	50	−21.3	11.1	−43.6	0.8	−1.8	4.0	−11.8	14.4
	SaT	27	−17.1	8.5	−35.2	−0.4	−0.3	4.2	−9.0	6.0
	TZ	19	−17.7	7.6	−36.3	−2.5	6.7	6.1	−8.6	15.4
	GC	29	−23.0	10.0	−46.4	−1.3	8.1	6.3	−7.6	17.0
	BC	30	n.m.*	n.m.*	n.m.*	n.m.*	n.m.*	n.m.*	n.m.*	n.m.*
	YU	48	−22.1	8.8	−48.5	−2.2	10.1	5.9	−4.8	17.8
	YL	66	−20.8	7.2	−42.6	−4.5	9.2	5.6	−3.9	17.7
2011	CT	32	−22.1	9.6	−47.9	−0.7	−5.5	8.5	−20.3	13.6
	UT	30	−19.8	9.6	−42.5	1.7	−2.2	9.9	−22.4	12.4
	SaT	47	−16.6	7.6	−37.2	−2.7	0.6	7.8	−16.4	13.1
	TZ	34	−17.5	7.2	−35.3	−3.4	4.3	7.3	−10.5	16.4
	GC	44	−24.2	10.2	−45.1	−4.0	5.6	7.6	−11.5	17.5
	BC	46	−19.3	9.7	−29.6	−1.7	6.9	7.7	−8.6	21.3
	YU	55	n.m.*	n.m.*	n.m.*	n.m.*	n.m.*	n.m.*	n.m.*	n.m.*
	YL	69	−19.2	10.8	−41.6	0.1	6.6	7.4	−7.9	19.6
2012	CT	37	−24.3	7.3	−41.9	−6.1	−4.0	6.6	−15.9	10.3
	UT	36	−17.6	7.5	−45.3	2.0	2.1	7.9	−10.6	16.4
	SaT	40	n.m.*	n.m.*	n.m.*	n.m.*	n.m.*	n.m.*	n.m.*	n.m.*
	TZ	39	−20.9	7.6	−43.1	−6.3	3.9	6.6	−10.7	16.1
	GC	58	−25.9	9.7	−50.0	−8.3	5.8	6.5	−8.2	19.1
	BC	63	−13.7	6.5	−37.3	−5.7	6.5	7.3	−5.9	20.4
	YU	33	−21.1	11.2	−49.7	3.4	11.7	6.7	−6.9	23.8
	YL	73	−13.7	7.0	−38.2	7.2	7.9	6.6	−5.3	19.5

* n.m. denotes not measured.

to openings, and I calculated the area of the exposed soil using measured four-directional lengths. The oval shape (using averaged length from the east, west, and south sides as the length of the semi-major axis, and the north side as the length of the semi-minor axis) shows that the 2010 extents of exposed and snow-covered areas were 135 and 265 m^2 for TZ, and 102 and 298 m^2 for GC, respectively.

2.2 Estimation of soil CO_2 efflux

Using a portable chamber CO_2 efflux system, soil CO_2 efflux measurements were conducted during snow-covered and snow-melting periods to minimize artificial effects. As described in Kim et al. (2013), the measurement system consisted of a transparent-material chamber (24 cm in diameter and 8 cm in height); a stainless steel base (24 cm in diameter and 10 cm in height); input and output polyurethane-material tubing (6 mm outside diameter, 4 mm inside diameter; LI-COR. Inc., USA) and pressure vent; a micro pump (CM-15-12, Enomoto Inc., Japan) equipped with a mass flow meter (1 L min^{-1}); a Li-820 NDIR (nondispersive infrared) CO_2 analyzer (LI-COR. Inc., USA); a 12 V battery for power; and a laptop computer running software for calculations from the following Eq. (1). Nine chamber bases were inserted into the soils of boreal forest sites during spring. To prevent contamination and disturbance, the bases were not used at boreal sites during snow-covered periods due to the soft snow surface (Kim et al., 2007, 2013). Bases were used to measure soil CO_2 efflux when the snow surface was hardened by sublimation at the tundra sites. Because of the extremely colder ambient temperature in January 2010 (e.g., < 30 °C), the NDIR analyzer shut down, and winter CO_2 efflux and soil temperature were not measured.

Flux measurement times were at 5–10 min intervals, depending on local weather and soil surface conditions, and efflux was calculated using the following equation, as described by Kim et al. (2013):

$$F_{CO_2} = \rho_a \cdot (C/t) \cdot (V/A), \quad (1)$$

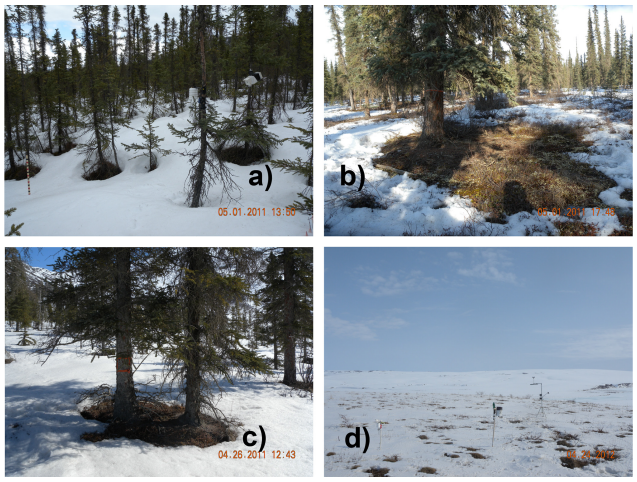

Figure 2. Site views at the **(a)** black spruce forest site (BC); **(b, c)** white spruce sites (GC and TZ); and **(d)** tundra site (UT) during spring of 2011. Exposed soils were found in surrounding trunk wells **(a–c)** and in tussock **(d)** due to the fast melting of snow from nighttime long-wave radiation.

where ρ_a is the molar density of dry air (mol m^{-3}), C (ppmv – parts per million by volume) is the change in CO_2 concentration during the measurement period (t, 5–10 min), V is chamber volume, and A is surface area (cross section $= 0.28\,m^2$). The pump was maintained at a flow rate of 1.0 L min^{-1} to avoid underestimation or overestimation of carbon flux from the occurrence of under- and overpressurization between the inside and outside of the chambers (Savage and Davidson, 2003). The height of each chamber was also measured alongside the chamber to allow for efflux calculation.

To estimate the response from temperature dependence on soil CO_2 efflux, the relationship was plotted, showing exponential curves on soil temperature at 5 cm depth from the equation

$$CO_2 \text{ efflux} = \beta_0 \cdot e^{\beta 1 \cdot T}, \quad (2)$$

where CO_2 efflux is the measured soil CO_2 efflux (gC m^{-2} day^{-1}), T is soil temperature (°C), and β_0 and β_1 are constants. This exponential relationship is commonly used to represent soil carbon flux as a function of temperature (Davidson et al., 1998; Xu and Qi, 2001; Davidson and Janssens, 2006; Rayment and Jarvis, 2000; Kim et al., 2007, 2013). Q_{10} temperature coefficient values were calculated as in Davidson et al. (1998) and Kim et al. (2013):

$$Q_{10} = e^{\beta_1 \cdot 10}, \quad (3)$$

where Q_{10} is a measure of the change in reaction rate at intervals of 10 °C and is based on van 't Hoff's empirical rule that a rate increase of 2–3 times occurs for every 10 °C rise in temperature (Lloyd and Taylor, 1994).

Soil temperature at 5 cm below the surface, in conjunction with the soil CO_2 efflux measurement, was measured at each site with a portable thermometer (model 8402-20, Cole-Palmer, USA). For additional measurements of soil temperature, hourly temperatures at depths of 5, 10, and 20 cm, and at 1.3 m above ground (HOBO data logger U-12 and sensor TMC6-HD, Onsetcomp, USA) were monitored at each site.

A one- or two-way ANOVA (analysis of variance; 95 % confidence level) and regression analysis of data using Microsoft Excel Data Analysis software were also performed.

3 Results and discussion

3.1 Estimation of winter and spring soil CO_2 efflux

During winter, the average and standard deviations for winter CO_2 efflux at boreal forest and tundra sites were 0.18 ± 0.07 (coefficient of variation, CV: 39 %) and 0.11 ± 0.10 (CV: 91 %) gC m^{-2} day^{-1} during 2011, and 0.22 ± 0.11 (CV: 50 %) and 0.05 ± 0.11 (CV: 220 %) gC m^{-2} day^{-1} during 2012, respectively. Average soil temperature at 5 cm in boreal forest and tundra were -8.3 ± 1.8 (CV: 22 %) and -12.7 ± 2.9 (CV: 23 %) °C, respectively, during 2011, and -3.8 ± 1.4 (CV: 37 %) and -14.4 ± 12.8 (CV: 89 %) °C, respectively, during 2012. Furthermore, during the winter season, snowpack CO_2 concentration gradients in snowpack between trees and near tree wells were 2.52–4.78 ppm cm^{-1} and 0.93–1.20 ppm cm^{-1}, measured using a stainless-steel-made probe (0.4 cm OD; 0.2 cm ID; 80 cm long) with connecting tubing, tri-way stopcock, and syringe at subsurface and bottom snowpack depths, respectively. This suggests that a lower CO_2 gradient near the tree trunk results in faster CO_2 transport from the soil through snowpack to the atmosphere than through snowpack between trees. This demonstrates that the air–snow–soil interface surrounding the tree trunk is much thinner than in forest opening areas.

For the end of the winter season, the 3-year average snow depth in boreal forest and tundra were 51.2 ± 15.3 (CV: 30 %) cm, and 36.0 ± 8.6 (CV: 24 %) cm respectively, as shown in Table 2. Winter CO_2 efflux depends on soil temperature at 5 cm below the surface, a depth at which the relationship equation amounts to winter CO_2 efflux $= 0.42 \cdot e^{(0.126 \cdot ST5)}$ ($R^2 = 0.82$; $Q_{10} = 3.5$; $p < 0.001$; not shown).

During spring, average CO_2 effluxes in exposed and snow-covered soils were 1.31 ± 0.25 (CV: 20 %) and 0.17 ± 0.18 (108 %) gC m^{-2} day^{-1} in 2010, 5.38 ± 3.67 (69 %) and 0.30 ± 0.33 (110 %) gC m^{-2} day^{-1} in 2011, and 2.71 ± 1.77 (65 %) and 0.27 ± 0.20 (74 %) gC m^{-2} day^{-1} in 2012, respectively. Because the snow-disappearance date in 2011 was approximately 10–17 days earlier than in both 2010 and 2012, based on 4 h time-lapse camera measurements, and the spring CO_2 efflux in exposed soils in 2011 was at least tenfold higher than in snow-covered soils.

The 3-year average spring CO_2 effluxes in four directions within the white spruce forest were 3.87 ± 4.45 (CV: 115 %) $gC\,m^{-2}\,day^{-1}$ to the east, 3.00 ± 3.60 (CV: 120 %) $gC\,m^{-2}\,day^{-1}$ to the west, 4.64 ± 4.61 (CV: 91 %) $gC\,m^{-2}\,day^{-1}$ to the south, and 1.25 ± 2.46 (CV: 197 %) $gC\,m^{-2}\,day^{-1}$ to the north, respectively, at the GC site. At TZ, average effluxes were 2.40 ± 2.60 (CV: 108 %) $gC\,m^{-2}\,day^{-1}$ to the east, 2.31 ± 2.53 (CV: 109 %) $gC\,m^{-2}\,day^{-1}$ to the west, 3.00 ± 3.12 (CV: 104 %) $gC\,m^{-2}\,day^{-1}$ to the south, and 1.50 ± 1.66 (CV: 110 %) $gC\,m^{-2}\,day^{-1}$ to the north. The magnitude of snow disappearance depends on solar radiation and the strength of long wavelengths from the tree trunk at nighttime during the spring. The much wider exposed area showed south $>$ east and west $\gg$ north, in turn, from trunks in the white spruce forest. The average diameter at breast height (DBH; 18 ± 4.5 cm) for white spruce is much thicker than for black spruce (DBH 5.8 ± 3.2 cm), suggesting that the difference in radiation uptake and heat emission capacity between both forests resulted in that of dent size, as shown in Fig. 2a–c. This feature is thought here to be related to the differences in exposed extent and soil CO_2 production within boreal forest sites.

In the tundra ecosystem, during the spring, seasonally covered snowpack began its melt in the tussock tundra, indicating shallower snowpack and vascular plants at the tussock top (e.g., *Eriophorum vaginatum*) that are vulnerable to strong solar radiation, as shown in Fig. 2d. Soil CO_2 efflux in exposed tussock tundra appeared to be more than tenfold greater than in seasonally snow-covered tundra, ranging from $0.13 \pm 0.09\,gC\,m^{-2}\,day^{-1}$ in 2011 to $1.46 \pm 1.07\,gC\,m^{-2}\,day^{-1}$ in 2010. Furthermore, Kim et al. (2007) demonstrated that winter CO_2 efflux in tussock was much higher than in the sphagnum moss of a black spruce forest of interior Alaska. This suggests that the vascular plants at the top of the tussock acted as a conduit in transporting soil-originated CO_2 through vascular plants and snowpack to the atmosphere (Kim et al., 2007). Oechel et al. (1997) also suggested that the winter carbon flux in moist tussock tundra was $0.3\,gC\,m^{-2}\,day^{-1}$ – much higher than the $0.08\,gC\,m^{-2}\,day^{-1}$ of coastal wet sedge ecosystems. In upland tussock tundra, the spring CO_2 efflux ($\sim 1.0\,gC\,m^{-2}\,day^{-1}$) was much higher than in other vegetation communities of the Alaska tundra (Fahnestock et al., 1998). A moist tussock ecosystem is a significant soil-originated carbon source during winter and spring seasons. Therefore, the contributions from winter/spring tussock-originated carbon efflux to the atmospheric carbon source are significant for understanding regional carbon budget responses to changes in phenology (Post et al., 2013), the cryosphere environment (AMAP, 2011), and shrub abundance (Sturm et al., 2005) under recent climate warming in the Arctic.

3.2 Dependence of temperature on soil CO_2 efflux

Average soil temperature at 5 cm depth tends to be higher in boreal forest soils than in tundra soils, as most of the tundra sites were still experiencing compacted snowpack and strong sublimation effects, except for the tussock tundra regime. Snow depth was nevertheless deeper over the boreal forest than the tundra; however, the density of the snow column was slightly higher in the tundra ($0.15 \pm 0.02\,g\,m^{-3}$) than in the boreal forest ($0.13 \pm 0.02\,g\,m^{-3}$) for 2010. Thus, compacted snow-covered tundra soils took longer to melt than in boreal forests, suggesting the tundra sites maintained a longer below-zero point than boreal forests. Furthermore, shallower snow-covered soils surrounding tree stems and tussock are susceptible to quickly denude from ablation rings, as shown in Fig. 2. Average soil temperature at 5 cm in 2011, then, was higher than in 2010 and 2012 in the exposed and snow-covered soils of the boreal forest and tundra. Furthermore, the response of the soil CO_2 efflux to soil temperature at 5 cm showed an exponential curve in these boreal forest and tundra (Fig. 3), indicating a surge in soil CO_2 efflux when soil temperature changed from below to above zero. This may be the result of enhanced soil microbial activity upon an increase in soil temperature just after the snowpack had disappeared. Hence, soil temperature is clearly a significant factor in determining winter/spring soil CO_2 efflux, as reported by many researchers. As shown in Fig. 3, the range in soil temperature differs greatly, indicating seasonal snow-disappearance timing. This further demonstrates that soil CO_2 efflux is constrained by seasonal snowpack below zero and is stimulated within exposed soil above zero. In particular, the soil CO_2 efflux ($> 10\,gC\,m^{-2}\,day^{-1}$) within white spruce forest sites in 2011 corresponds to the summer soil CO_2 efflux (Fig. 3b). Mikan et al. (2002) found that the temperature response from CO_2 efflux was related to soil organic matter (SOM) quality and soil microbial community in thawed tundra soils. Thus, higher spring efflux in the white spruce forest may result from accumulated SOM quality and the decomposition of preferentially labile carbon by soil microbes in exposed soils. As a result, spring soil CO_2 efflux must be assessed for its contribution to annual soil carbon efflux, in spite of the change in snow disappearance and spring season timing (Richter et al., 2000). The relatively higher CO_2 efflux in tussock tundra soils is above $0.75\,gC\,m^{-2}\,d^{-1}$, whereas it is below $0.50\,gC\,m^{-2}\,d^{-1}$ of snow-covered intertussock soils, as is shown in Fig. 3c. When soil temperature was above zero at the white spruce forest sites (Fig. 3b), spring soil CO_2 efflux greatly varied spatially; however, this variation was due to data being obtained at four directional sides from the trunk, as described in Sect. 3.1.2 (see Fig. 2). Hence, the magnitude of spring CO_2 efflux is determined by soil temperature at 5 cm depth below or above zero, indeed reflecting the stimulation of soil microbial activity with or without seasonally covered snowpack. Mikan et al. (2002) demonstrated that the temperature response in frozen and thawed tundra soils

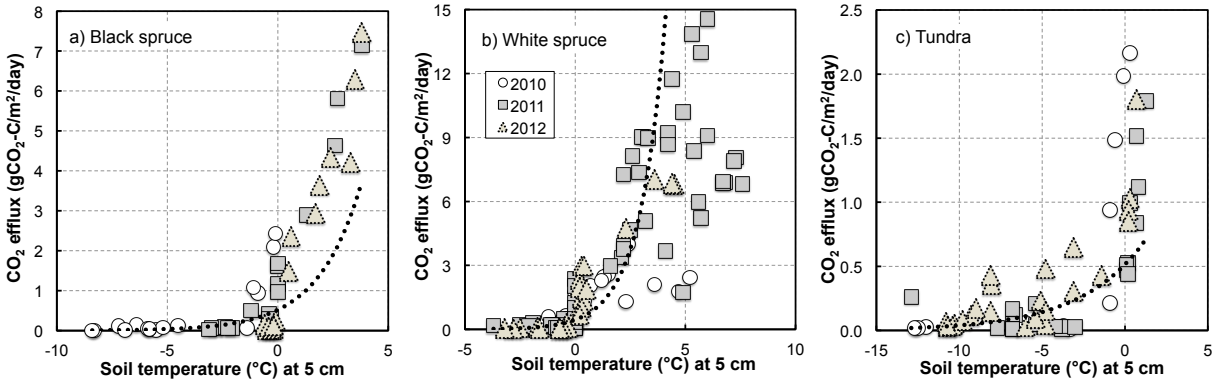

Figure 3. Spring CO_2 efflux responses to soil temperature at 5 cm below the surface at **(a)** black spruce forest sites; **(b)** white spruce forest sites; and **(c)** tundra sites, during the spring of 2010–2012. Dotted curves denote the 3-year exponential relationship between spring CO_2 efflux and soil temperature.

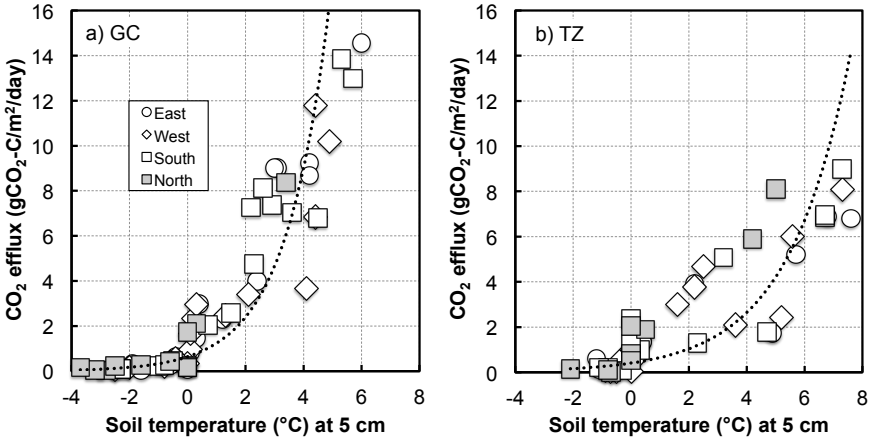

Figure 4. Spring CO_2 efflux responses to soil temperature at 5 cm below the surface, measured in four directions from the stem of white spruce at **(a)** GC and **(b)** TZ sites during the spring. Dotted curves denote the 3-year exponential relationship between spring CO_2 efflux and soil temperature.

was displayed differently through a culture experiment above and below 0 °C, as the unfrozen water content in frozen soil, which is a significant controlling factor, greatly affected the physiological response of soil microbes, including extracellular and intercellular mechanisms. However, unfrozen water was also unrelated to soil organic matter quality, as well as the nutrients contained in tundra organic soils (Mikan et al., 2002). These results are beneficial to better understanding the temperature response from spring CO_2 efflux to below and above freezing temperatures in tundra and boreal forest soils.

The response of spring soil CO_2 efflux at white spruce forest sites (e.g., GC and TZ) to soil temperature at 5 cm is shown in Fig. 4. Q_{10} values at GC and TZ sites ranged from 414 west to 1003 south, and from 43 west to 658 north, respectively. Furthermore, the Q_{10} value was 2.6×10^5 at black spruce forest sites during the spring of 2011, as shown in Table 3.

Within the tundra ecosystem (Fig. 3c), although soil temperature was below zero, soil CO_2 efflux was quite higher. This may be due to both (1) a shallower thawed soil surface (less than 5 cm) and (2) the absorption of solar radiation by exposed plants (see Fig. 2d). It was difficult to measure soil temperature near the soil surface with the portable thermometer in these situations. The response of spring soil CO_2 efflux to soil temperature at 5 cm depth in the upland tussock tundra was CO_2 efflux $= 1.22 \cdot e^{(0.15 \cdot ST5)}$ ($R^2 = 0.43$; $Q_{10} = 4.4$; not shown). However, during the winter seasons of 2010–2012, the equations for winter soil CO_2 efflux and soil temperature at 5 cm depth over the entire tundra and tussock tundra were CO_2 efflux $= 1.57 \cdot e^{(0.294 \cdot ST5)}$ ($R^2 = 0.62$; $Q_{10} = 19.0$; not shown) and CO_2 efflux $= 75.4 \cdot e^{(0.64 \cdot ST5)}$ ($R^2 = 0.59$; $Q_{10} = 605$; not shown), respectively. Q_{10} values from Eq. (3) were calculated at boreal forest and tundra sites, as shown in Table 3.

Table 3. Constants and correlation coefficients in the exponential equation for soil CO_2 efflux response to soil temperature at 5 cm below the surface in white spruce, black spruce, and tundra sites across the haul road of Alaska during the spring seasons of 2010–2012, for which the equation is CO_2 efflux $= \beta_0 \cdot e^{(\beta 1 \cdot T)}$, based on a one-way ANOVA at the 95 % confidence level.

Year	Number	Whole					White spruce					Black spruce					Tundra				
		β_0	β_1	R^2	Q_{10}*	p	β_0	β_1	R^2	Q_{10}*	p	β_0	β_1	R^2	Q_{10}*	p	β_0	β_1	R^2	Q_{10}*	p
2010	49	1.064	0.373	0.90	41.7	< 0.001	0.766	0.343	0.53	31	0.075	1.414	0.588	0.77	358	0.0125	0.588	0.310	0.59	22.2	0.0030
2011	100	0.890	0.337	0.61	29.1	< 0.001	0.530	0.506	0.73	158	0.002	0.664	0.841	0.90	4492	0.0083	0.379	0.290	0.40	18.2	< 0.001
2012	67	0.889	0.282	0.72	16.8	0.0015	0.448	0.851	0.66	4964	0.007	0.143	1.248	0.77	263 024	< 0.001	0.793	0.254	0.62	12.7	< 0.001
Total	216	0.937	0.328	0.72	26.6	< 0.001	0.525	0.531	0.67	202	< 0.001	0.522	0.512	0.72	167	< 0.001	0.515	0.256	0.45	12.9	< 0.001

* Q_{10} is calculated from Eq. (3).

Higher Q_{10} values for the winter and spring seasons were found within boreal white and black spruce forests, and tundra sites across the Dalton Highway, compared to Q_{10} values of 2.1–18 from the growing season (Kim et al., 2013). The possibility that Q_{10} values during winter and spring were much higher than during the growing season would suggest the exponential growth of microbes (e.g., snow molds), considering that beneath-snowpack soils warming from −3 to 0 °C have also been shown to have higher CO_2 production in a high-elevation, subalpine forest within the Colorado Front Range (Rocky Mountains) (Monson et al., 2006a, b; Schmidt et al., 2009). Monson et al. (2006a, b) demonstrated that soil microbes' beneath-snow CO_2 efflux response (e.g., Q_{10} value: 105–1.25 × 10^6) corresponded to a narrower range of soil temperature (−1.0 to 0.0 °C). Furthermore, the drastic increase in CO_2 efflux was induced by a strong response from beneath-snow microbes, with a much higher dependence from microbial biomass upon an increase in soil temperature in the late winter and early spring seasons (Schmidt et al., 2009). In this study, two colonies of unidentified fungi on cryoturbed soils within the chamber base were found at the UT site on 18 April 2010, as shown in Fig. 5, and the soil CO_2 efflux was not much higher than expected, due to the dehydrated fungi. Nevertheless, a Q_{10} value of 4.2 × 10^6 remained the highest in the exposed tussock tundra and cryoturbed soils of the UT site, reflecting a sharp rise in soil CO_2 efflux (0.5–2.2 g C m^{-2} day^{-1}) as tundra soils warmed from −0.9 to 0.5 °C. While acknowledging the important role of saprotrophic snow molds in forming a dense hyphal mat, and showing high levels of subnivean respiration in alpine forests (Monson et al., 2006a, b), the snow fungi found in this study disappeared within days of the soils becoming snow-free (Schmidt et al., 2007), as shown in Fig. 5, and did not produce high CO_2 efflux due to dehydration in spring.

Fungi are omnipresent in Arctic and subarctic soils, where they function as plant symbionts, parasites, pathogens, and decomposers, and may affect the carbon balance of terrestrial ecosystems subjected to climate change in the Arctic (Timling and Taylor, 2012). For example, Panikov et al. (2006) demonstrated evidence that soil CO_2 was produced by microbial activity even at the extremely low temperature of −39 °C in Arctic soils from Barrow, western Siberia, and Sweden. Furthermore, it has been widely shown that microbial metabolism occurs in Arctic, subarctic, and subalpine soils under seasonally covered snowpack, even at soil temperatures below 0 °C (Sommerfeld et al., 1993; Brooks et al., 1996; Oechel et al., 1997; Winston et al., 1997; Fahnestock et al., 1998; Monson et al., 2006a, b; Schmidt et al., 2007; Kim et al., 2007, 2013; Björkman et al., 2010). Microbial activity in the cold soils of the Arctic and subarctic is a significant key in determining the susceptibility of old-aged soil organic carbon from a deepening active layer and thawing permafrost in response to Arctic warming (Marchenko et al., 2008; Ping et al., 2008; Tarnocai et al., 2009; Grosse et al., 2011).

Figure 5. The unidentified fungi colonies (red circles) within the chamber base found on the cryoturbed soils of the UT site on 18 April 2010.

3.3 Effect of snow depth and snow crust

In contrast to soil temperature, snow depth is not significantly related to the determination of spring CO_2 efflux, as in Fig. 6a, such that the exponential and linear equations for tundra sites during the spring season are CO_2 efflux $= 0.43 \cdot e^{(-0.054 \cdot ST5)}$ ($R^2 = 0.22$) and CO_2 efflux $= -0.02 \cdot ST5 + 0.83$ ($R^2 = 0.27$), respectively. This suggests CO_2 efflux is produced by soil microbial activity in snow-covered tundra soils. The lowest temperature with detectable

CO_2 production was −39 °C in tundra soils (Panikov et al., 2006), reflecting seasonal changes in the abundance of cold tolerance microbes in tundra soils. During winter and early spring seasons, Fahnestock et al. (1998) reported that the response from CO_2 efflux to snow depth was quietly weak among vegetation community types of Alaska tundra, representing a correlation coefficient of $R^2 = 0.18$. Although snow depth is not an important key in influencing winter and spring CO_2 efflux in the tundra ecosystem, it does have a significant effect on the tall shrub community, as deep snowpack provides better insulation for stimulating CO_2 efflux from the soil (Sturm et al., 2005). Hence, additional research is needed not only to observe soil temperature in deep and shallow snow accumulation areas, but also to monitor soil CO_2 efflux using a simple forced diffusion (FD) chamber method (Risk et al., 2011).

Meanwhile, snow crust is formed by strong winds and is found across snowpack pit-wall observations in the Arctic. The characteristics of this crust correspond to the horizontal ice layer in temperate regions. Several researchers have suggested that ice layers within the snowpack may have a significant effect on CO_2 transport from seasonally snow-covered soils (Hardy et al., 1995; Winston et al., 1997). Mast et al. (1998) suggested that horizontal ice layers had a considerably lower CO_2 diffusivity than the surrounding snow, but did not block CO_2 efflux from the snowpack surface in the subalpine soils of Colorado. These authors described no effect from ice layers for estimating winter CO_2 efflux, as the concentration gradients above and below these layers were almost linearly the same. CO_2 efflux after the removal of snow crust is much higher – by 2.8–28 times – than before the removal, suggesting that snow crust likely does play a role in blocking CO_2 transport through the snowpack to the atmosphere over the North Slope of Alaska. As shown in Fig. 6b, the relationship between CO_2 efflux and soil temperature at 5 cm, with and without snow crust, were CO_2 efflux $= 0.10 \cdot e^{(0.18 \cdot ST5)}$ ($R^2 = 0.27$; $Q_{10} = 6.0$) and CO_2 efflux $= 0.98 \cdot e^{(0.31 \cdot ST5)}$ ($R^2 = 0.29$; $Q_{10} = 23$), respectively. Although continuous CO_2 efflux measurement was not conducted in spring, once the seasonally covered snowpack begins to melt, the CO_2 trapped beneath the snow crust will eventually be released to the atmosphere.

3.4 Implications for spring CO_2 emission

The response from spring CO_2 efflux to soil temperature at 5 cm below the soil surface at all sites during the spring seasons of 2010–2012 is shown in Fig. 7. The relevant equations here are CO_2 efflux $= 1.06 \cdot e^{(0.373 \cdot ST5)}$ ($R^2 = 0.90$; $Q_{10} = 41.7$; $p < 0.001$) in 2010, CO_2 efflux $= 0.89 \cdot e^{(0.337 \cdot ST5)}$ ($R^2 = 0.62$; $Q_{10} = 29.1$; $p < 0.001$) in 2011, and CO_2 efflux $= 0.89 \cdot e^{(0.282 \cdot ST5)}$ ($R^2 = 0.72$; $Q_{10} = 16.7$; $p = 0.0015$) in 2012, respectively. Furthermore, the 3-year average equation is CO_2 efflux $= 0.94 \cdot e^{(0.328 \cdot ST5)}$ ($R^2 = 0.72$; $Q_{10} = 26.7$; $p < 0.001$) across the tundra and boreal forest during the spring seasons of 2010–2012. The 3-year spring CO_2 efflux shows spatial distribution across 66–70° N, along the Dalton Highway, with latitudinal distribution of soil temperature at 5 cm. In reality, since the northernmost CT site was experiencing the winter season at the designated measurement time, this does not represent strict spring season data. However, this study may be used to estimate spring CO_2 efflux in exposed and snow-covered soils of tundra and boreal forest, while excluding the northernmost site. As shown in Fig. 7, higher efflux is indicated in white spruce forest sites, at $> 5\,gC\,m^{-2}\,day^{-1}$, reflecting an ablation ring effect. Hardy et al. (1995) and Winston et al. (1997) further suggested that soil CO_2 efflux from a tree well showed results tenfold higher than for forest openings. That is, there is a clear difference in spring CO_2 efflux between a tree trunk in exposed soils and a forest opening in seasonally snow-covered soils. Furthermore, using a FLIR (forward looking infrared) camera on the North Slope during the mid-winter season (Yoshikawa, unpublished data), the temperature within tussock tundra showed relatively higher results (−35.5 °C) than in the intertussock (< −42.7 °C). IR (infrared) camera and visual photos were taken over tussock tundra at the white spruce forest site (TZ) on 19 April 2010, as shown in Fig. 8 (image courtesy of H. Enomoto), demonstrating an obvious difference in temperature between the top of the tussock and the snow surface. Moreover, temperatures at the top of the tussock and in the intertussock were monitored at the UT site from 28 August 2010 to 11 July 2012, as shown in Fig. 9. The temperature difference between the top of the tussock and the intertussock was displayed distinctly during the spring seasons of 2011 and 2012. This mechanism is identical to the ablation effect in boreal forests, as shown in Fig. 2. This result from strong solar radiation in daytime was similar to that which occurred in the exposed tussock top. Interestingly, the temperature difference between the two steadily increased with time. Most temperature features at the top are likely to be affected by changes in ambient temperature due to geographical relief, and showed much greater differences during the springs of 2011 and 2012, as well as during the early winter of 2012. This suggests that spring-season CO_2 efflux from tussock tundra depended on the temperature of tussock tundra during 2011 and 2012. Hence, tussock tundra represented a significant carbon source for the tundra ecosystem during winter and spring for the estimation of seasonal and annual Arctic carbon budgets (Oechel et al., 1997; Fahnestock et al., 1998, 1999; Kim et al., 2007, 2013).

Growing season CO_2 efflux measurements were conducted at each site, from August to September of 2010, for contributions from winter and spring CO_2 emissions to the annual carbon budget. However, as efflux could not be measured during 2011 and 2012, due to rainy and cold weather conditions in the late fall season (i.e., late September–early October), the calculation of seasonal emissions used data observed in 2010 and by Kim et al. (2013). Furthermore, the contribution of average 3-year winter and spring CO_2

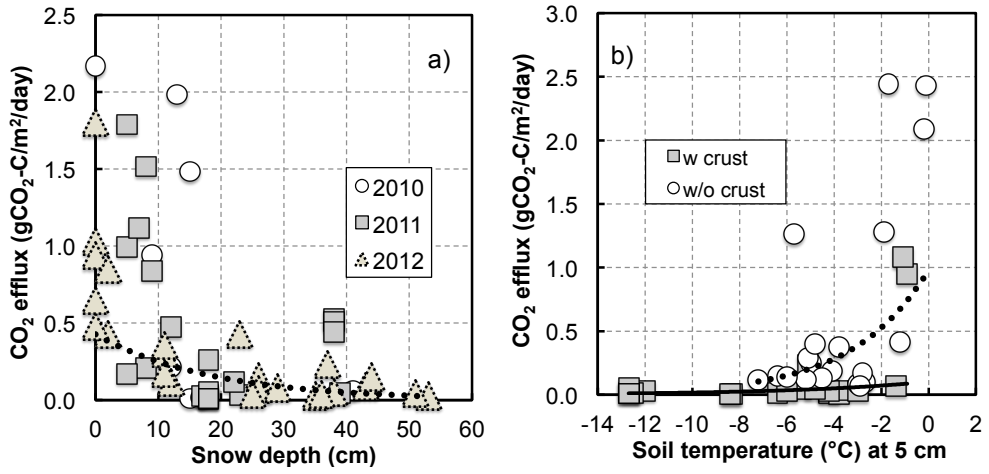

Figure 6. Spring CO_2 efflux responses to **(a)** snow depth and **(b)** soil temperature at 5 cm below the surface, with and without snow crust at tundra sites during the spring. Dotted and solid curves denote the 3-year exponential relationship between spring CO_2 efflux and **(a)** snow depth and **(b)** soil temperature, before and after cluster removal.

Table 4. Contributions (%) from seasonal CO_2 emissions to the annual carbon budget in tundra and boreal forest ecosystems, under the average seasonal period during 2010 and 2011*.

Ecosystem	Season	2010		2011*		2012*		Period
		CO_2 emission $gC\,m^{-2}$	Contribution %	CO_2 emission $gC\,m^{-2}$	Contribution %	CO_2 emission $gC\,m^{-2}$	Contribution %	days
Tundra	Winter	33	14	45	17	28	12	250
	Spring	46	20	72	27	47	21	60
Boreal forest	Winter	61	9	95	11	63	8	180
	Spring	108	16	264	31	176	24	80

* Summer CO_2 emissions of 2011 and 2012 were used by the average of 2010 data and Kim et al. (2013).

emissions to the atmosphere corresponds to roughly 14–22 % for tundra and 9–24 % for boreal forest sites, of the total annual carbon respired, using data from both the 2010 growing season and Kim et al. (2013), as shown in Table 4. Winter CO_2 contributions to annual carbon emissions within tundra, alpine, and boreal forest ecosystems range from 17 % for Alaskan tundra (Fahnestock et al., 1998) to > 25 % for alpine and subalpine regions (Sommerfeld et al., 1993), as reported by many researchers, suggesting that the results of this study are comparable with others. However, spring CO_2 contributions for the boreal forest reached up to almost 50 % of total annual carbon emissions, demonstrating the strong tree-well effect (Hardy et al., 1995; Winston et al., 1995, 1997) of the boreal forest, as well as the significance of tussock tundra (Oechel et al., 1997; Fahnestock et al., 1998, 1999; Kim et al., 2007) in tundra and boreal forest ecosystems.

Considering the ablation ring effect for white spruce forest sites, the CO_2 effluxes in the spring, winter, and summer seasons of 2010 were 1.8, 0.6, and 3.6 $gC\,m^{-2}\,day^{-1}$ for TZ, respectively, and 2.4, 0.4, and 2.8 $gC\,m^{-2}\,day^{-1}$ for GC, respectively. Summer season CO_2 emissions, based on a 400 m^2 area, are shown in Table 5, corresponding to 4, 3, and 93 % of the annual carbon budget for TZ; and 5, 3, and 92 % for GC. Using 2010 soil CO_2 data, contributions to the annual carbon budget from spring, winter, and summer CO_2 emissions in the two white spruce forest sites during 2011 and 2012 are shown in Table 5. This feature suggests that the wider the extent of exposed soil, the greater the contribution to the annual carbon budget, based on a constant area. Although up to 5 % may sound small, this estimation could very well change the estimation for NEE (net ecosystem exchange) from a sink to a source.

4 Conclusions

Here, soil CO_2 efflux measurements were conducted at three tundra sites and five boreal forest sites along the Dalton Highway, during the winter and spring seasons of 2010–2012, for the estimation of spring CO_2 efflux and the corroboration of environmental factors determining efflux.

At boreal forest sites, tree trunks played significant roles in the disappearance of seasonal snowpack. Just after snowmelt, the 3-year spring CO_2 efflux in exposed soils is

Table 5. Contributions (%) from seasonal CO_2 emission contributions to the annual carbon budget, on the basis of a constant area (400 m^2) for the white spruce forest TZ and GC sites during the period 2010–2012*.

Site	Season	2010		2011**				2012**		Remarks
		May		April		May		May		
		CO_2 emission $gC\,d^{-1}$	Contribution %	CO_2 emission $gC\,d^{-1}$	Contribution %	CO_2 emission $gC\,d^{-1}$	Contribution %	CO_2 emission $gC\,d^{-1}$	Contribution %	
TZ	Winter	145	3	46	1	18	1	32	1	Snow-covered
	Spring	241	4	301	5	1978	27	56	1	Exposed
GC	Winter	121	3	90	2	81	1	35	1	Snow-covered
	Spring	246	5	316	7	1241	23	815	16	Exposed

* After the forest census in TZ and GC sites by Suzuki et al. (2013), the calculation used was the tree density within a 20 m × 20 m area. ** Summer 2010 CO_2 efflux was used in 2011 and 2012 due to late fall observation as described in the text.

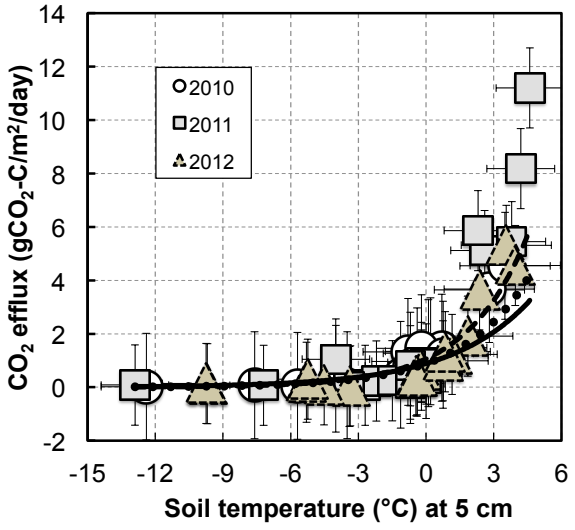

Figure 7. Spring CO_2 efflux responses to soil temperature at 5 cm below the surface, across entire sites during the spring seasons of 2010 and 2012. Dashed, dotted, and solid curves show 2010, 2011, and 2012, respectively.

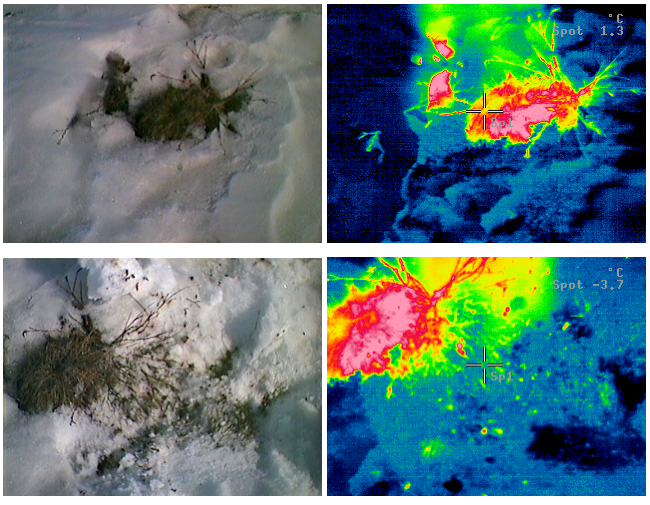

Figure 8. IR camera temperatures denote 1.3 °C at the top of tussock and −3.7 °C at the snow surface at the TZ site on 19 April 2010, suggesting a sharp difference between the tussock top and the snow surface (image courtesy of H. Enomoto).

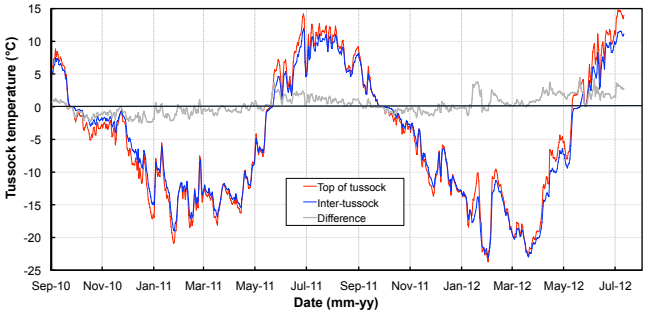

Figure 9. Temporal temperature variations for the top of tussock (red), the intertussock (blue), and the temperature difference (gray) between the two at the UT site from 28 August 2010 (DOY 240) to 11 July 2012 (DOY 923).

tenfold higher than in snow-covered soil, corresponding to growing-season CO_2 efflux. Spring CO_2 efflux represents dependence on soil temperature at 5 cm below the surface, accounting for 67 and 72 % of the variability of spring CO_2 efflux in white and black spruce forest soils, respectively. Efflux indicates south > east and west ≫ north, in turn, in four directions from tree trunks in the white spruce forest, attributing the magnitude of spring CO_2 efflux to the expansion of exposed soil by the difference in solar radiation.

At tundra sites, spring CO_2 efflux in exposed tussock tundra soils is much higher than in seasonally snow-covered soils, as reported by many scientists studying the North Slope of Alaska, which suggests that tussock tundra acts as an important conduit for transporting soil CO_2 through the snowpack, and is also a significant carbon source during winter and spring. Furthermore, the temperature at the top of tussock tundra is relatively higher than in the intertussock, indicating a clear difference in temperature during the snow-covered and snow-melting seasons of 2011 and 2012. Three-year average spring CO_2 efflux depends on soil temperature at 5 cm below the surface, explaining 45 % of the variability of spring CO_2 efflux in tundra soils.

Finally, the contribution of subnivean respiration from snow molds and fungi should be a critical issue to understanding carbon dynamics, as recent research results in subalpine, alpine, boreal forest, and tundra regions, suggest that microbial activity depends explicitly on soil temperature in the early spring season. Microbial activity in the cold soils of the Arctic and subarctic is a significant decomposer when assessing the vulnerability of old-soil organic carbon from a deepening active layer, as well as the degradation of permafrost in response to recent Arctic warming. Considering the distribution areas of tussock/moss in the high Northern Hemisphere (6.5×10^{12} m^2; Whalen and Reeburgh, 1998) and the acclimation of snow molds and fungi in polar environments (Tojo and Newshan, 2012), the contributions from tussock tundra and beneath-snowpack microbes in winter and spring seasons toward the soil CO_2 efflux outburst within a narrower range of soil temperatures should not be overlooked when estimating regional and pan-Arctic-scale carbon budgets.

Acknowledgements. This research was conducted under the IARC-JAXA Information System (IJIS) project with funding supported by the Japan Aerospace Exploration Agency (JAXA), and under the JAMSTEC-IARC Collaboration Study (JICS) with funding provided by the Japan Agency for Marine-Earth Science and Technology (JAMSTEC), through a grant to the International Arctic Research Center (IARC). We thank Dr. H. Enomoto of the National Institute of Polar Research (NIPR), Japan, for providing the IR images, and N. Bauer of the International Arctic Research Center (IARC) at the University of Alaska Fairbanks for constructive editorial revisions of the manuscript. Finally, I would like to acknowledge the handing editor (Yiqi Luo) and two anonymous reviewers who significantly improved the manuscript's quality and readability.

Edited by: Y. Luo

References

ACIA (Arctic Climate Impact Assessment): Impacts of a Warming Arctic, Cambridge Univ. Press, Cambridge, UK, 146 pp., 2005.

AMAP: Snow, Water, Ice and Permafrost in the Arctic (SWIPA): Climate Change and the Crtosphere, Arctic Monitoring and Assessment Programme (AMAP), Oslo, Norway, xii + 538 pp., 2011.

Bhatt, U. S., Walker, D. A., Raynolds, M. K., Comiso, J. C., Epstein, H. E., Jia, G., Gens, R., Pinzon, J. E., Tucker, C. J., Tweedie, C. E., and Webber, P. J.: Circumpolar arctic tundra vegetation change is linked to sea ice decline, Earth Interact., 14, 1–20, doi:10.1175/2010EI315.1, 2010.

Bhatt, U. S., Walker, D. A., Raynolds, M. K., Bieniek, P. A., Epstein, H. E., Comis, J. C., Pinzon, J. E., Tucker, C. J., and Polyako, I. V.: Recent declines in warming and vegetation greening trends over pan-Arctic tundra, Remote Sens., 5, 4229–4254, doi:10.3390/rs5094229, 2013.

Björkman, M. P., Morgner, E., Cooper, E. J., Elberling, B., Klemedtsson, L., and Björ, R.: Winter carbon dioxide effluxes from Arctic ecosystems: An overview and comparison of methodologies, Global Biogeochem. Cy., 24, GB0310, doi:10.1029/2009GB003667, 2010.

Bliss, L. C. and Matveyeva, N. V.: Circumpolar Arctic vegetation, in: Arctic Ecosystems in a Changing Climate, edited by: Chapin III, F. S., Jefferies, R. L., Reynolds, J. F., Shaver, G. R., and Svoboda, J., Academic Press, San Diego, 59–89, 1992.

Bond-Lamberty, B. and Thomson, A.: Temperature-associated increases in the global soil respiration record, Nature, 464, 597–582, 2010.

Brooks, P. D., Williams, M. W., and Schmid, S. K.: Microbial activity under alpine snowpacks, Niwot Ridge, Colorado, Biogeochemistry, 32, 93–113, 1996.

Chapin, F. S., McGuire, A. D., Randerson, J., Pielke, R., Baldocchi, D., Hobbie, S. E., Roulet, N., Eugster, W., Kashschke, E., Rastetter, E. B., Zimov, S. A., and Running, S. W.: Arctic and boreal ecosystems of western North America as components of the climate system, Glob. Change Biol., 6, 211–223, 2000.

Davidson, E. A. and Jassens, I. A.: Temperature sensitivity of soil carbon decomposition and feedback to climate change, Nature, 440, 165–173, 2006.

Davidson, E. A., Belk, E., and Boone, R. D.: Soil water content and temperature as independent or confounded factors controlling soil respiration in a temperate mixed hardwood forest, Glob. Change Biol., 4, 217–227, 1998.

de Jong, R., de Bruin, S., de Wit, A., Schaepman, M. E., and Dent, D. L.: Analysis of monotoneic greening and browning trends from global NDVI times-series, Remote Sens. Environ., 115, 692–702, 2011.

Eugster, W., Rouse, W., Pielke, R. A., McFadden, J. P., Baldocchi, D., Kittel, T. F., Chapin, F. S., Liston, G. E., Vidale, P. L., Vaganov, E., and Chambers, S.: Land-atmosphere energy exchange in Arctic tundra and boreal forest: available data and feedbacks to climate, Glob. Change Biol., 6, 84–115, 2000.

Fahnestock, J. T., Jones, M. H., Brooks, P. D., Walker, D. A., and Welker, J. M.: Winter and early spring CO_2 efflux from tundra communities of northern Alaska, J. Geophys., Res., 103, 29023–29027, 1998.

Fahnestock, J. T., Jones, M. H., and Welker, J. M.: Wintertime CO_2 efflux from Arctic soils: Implications for annual carbon budgets, Global Biogeochem. Cy., 13, 775–779, 1999.

Grosse, G., Harden, J., Turetsky, M., McGuire, A. D., Camill, P., Tarnocai, C., Frolking, S., Schuur, E. A. G., Jorgenson, T., Marchenko, S., Romanovsky, V., Wickland, K. P., French, N., Waldrop, M., Bourgeau-Chaves, L., and Striegl, R. G.: Vulnerability of high-latitude soil organic carbon in North America to disturbance, J. Geophys. Res., 116, G00K06, doi:10.1029/2010JG001507, 2011.

Hardy, J. P., Davis, R. E., and Winston, G. C.: Evolution of factors affecting gas transmissivity of snow in the boreal forest, in: Biogeochemistry of Seasonally Snow-Covered Catchments, edited by: Tonnessen, K. A., Williams, M. W., and Tranier, M., IAHS Publ., 228, 51–60, 1995.

Kim, Y., Ueyama, M., Nakagawa, F., Tsunogai, U., Tanaka, N., and Harazono, Y.: Assessment of winter fluxes of CO_2 and CH_4 in boreal forest soils of central Alaska estimated by the profile method and the chamber method: A diagnosis of methane emis-

sion and implications for the regional carbon budget, Tellus B, 59, 223–233, 2007.

Kim, Y., Kim, S. D., Enomoto, H., Kushida, K., Kondoh, M., and Uchida, M.: Latitudinal distribution of soil CO_2 efflux and temperature along the Dalton Highway, Alaska, Polar Science, 7, 162–173, 2013.

Kojima, K.: Contribution of snow dent around stem on the snowmelt rate in larch forest, Japan, Snow and Ice in Hokkaido, 20, 9–12, 2001 (in Japanese).

Lloyd, J. and Taylor, J. A.: On the temperature dependence of soil respiration, Funct. Ecol., 8, 315–323, 1994.

Mahecha, M. D., Reichstein, M., Carvalhais, N., Lasslop, G., Lange, H., Seneviratne, S. I., Vargas, R., Ammann, C., Arain, M. A., Cescatti, A., Janssens, I. A., Migliavacca, M., Montagnani, L., and Richardson, A. D.: Global convergence in the temperature sensitivity of respiration at ecosystem level, Science, 329, 838–840, 2010.

Marchenko, S., Romanovsky, V., and Tipenko, G.: Numerical modeling of spatial permafrost dynamics in Alaska, in: Proceedings of the Ninth International Conference on Permafrost, edited by: Kane, D. L. and Hinkel, K. M., Inst. of North. Eng., Univ. of Alaska Fairbanks, Fairbanks, 1125–1130, 2008.

Mast, M. A., Wickland, K. P., Striegl, R. T., and Clow, D. W.: Winter fluxes of CO_2 and CH_4 from subalpine soils in Rocky Mountain National Park, Colorado, Global Biogeochem. Cy., 12, 607–620, 1998.

McDonald, K. C., Kimball, J. S., Njoke, E., Zimmermann, R., and Zhao, M.: Variability in springtime thaw in the terrestrial high latitudes: monitoring a major control on the biospheric assimilation of atmospheric CO_2 with spaceborne microwave remote sensing, Earth Interact., 8, 1–23, 2004.

Mikan, C. J., Schimel, J. P., and Doyle, A. P.: Temperature controls of microbial respiration in arctic tundra soils above and below freezing, Soil Biol. Biochem., 34, 1785–1795, 2002.

Monson, R. K., Lipson, D. L., Burns, S. P., Turnipseed, A. A., Delany, A. C., Williams, M. W., and Schmidt, S. K.: Winter forest soil respiration controlled by climate and microbial community composition, Nature, 439, doi:10.1038/nature04555, 2006a.

Monson, R. K., Burns, S. P., Williams, M. W., Delany, A. C., Weintraub, M., and Lipson, D. L.: The contribution of beneath-snow soil respiration to total ecosystem respiration in a high-elevation, subalpine forest, Global Biogeochem. Cy., 20, GB3030, doi:10.1029/2005GB002684, 2006b.

Oechel, W. C., Vourlitis, G., and Hastings, S. J.: Cold season CO_2 emissions from arctic soils, Global Biogeochem. Cy., 11, 163–172, 1997.

Panikov, N. S., Flanagan, P. W., Oechel, W. C., Mastepanov, M. A., and Christensen, T. R.: Microbial activity in soils frozen to below −39 6∘C, Soil Biol. Biochem., 38, 785–794, 2006.

Parent, M. B. and Verbyla, D.: The browning of Alaska's boreal forest, Remote Sens., 2, 2729–2747, 2010.

Ping, C.-L., Michaelson, G. J., Jorgenson, M. T., Kimble, J. H., Epstein, H., Romanovsky, V., and Walker, D. A.: High stock of soil organic carbon in the North American Arctic region, Nat. Geosci., 1, 615–619, doi:10.1038/ngeo284, 2008

Post, E., Bhatt, U. S., Bitz, C. M., Brodie, J., Fulton, T. L., Hebblewhite, M., Kerby, J., Kutz, S., Stirling, J. K., and Walker, D. A.: Ecological consequences of Sea-ice decline, Science 341, 519, doi:10.1126/science.1235225, 2013.

Raich, J. W. and Schlesinger, W. H.: The global carbon dioxide flux in soil respiration and its relationship to vegetation and climate, Tellus B, 44, 81–99, 1992.

Rayment, M. B. and Jarvis, P. G.: Temporal and spatial variation of soil CO_2 efflux in a Canadian boreal forest, Soil Biol. Biochem., 32, 35–45, 2000.

Raynolds, M. K., Walker, D. A., and Maier, H. A.: Alaska arctic tundra vegetation map. Scale 1:4,000,000. Conservation of Arctic Flora and Fauna (CAFF) Map No. 2, U.S. Fish and Wildlife Service, Anchorage, Alaska, 2006.

Richter, D. D., O'Neil, K. P., and Kasischke, E. S.: Postfire stimulation of microbial decomposition in black spruce (*Picea mariana L.*) forest soils: A hypothesis, in: Fire, Climate Change, and Carbon Cycling in the Boreal Forest, edited by: Kasischke, E. S. and Stock, B. J., Springer-Verlag, New York, 197–213, 2000.

Risk, D., Nickerson, N., Creelman, C., McArthur, G., and Owens, J.: Forced diffusion soil flux: A new technique for continuous monitoring of soil gas efflux, Agr. Forest Meteorol., 151, 1622–1631, 2011.

Savage, K. E. and Davidson, E. A.: A comparison of manual and automated systems for soil CO_2 flux measurements: trade-offs between spatial and temporal resolution, J. Exp. Bot., 54, 891–899, 2003.

Schlesinger, W. H. and Andrews, J. A.: Soil respiration and the global carbon cycle, Biogeochemistry, 48, 7–20, 2000.

Schmidt, S. K., Costello, E. K., Nemergut, D. R., Cleveland, C. C., Reed, S. C., Weitraub, M. N., Meyer, A. F., and Martin, A. M.: Biogeochemical consequences of rapid microbial turnover and seasonal succession in soil, Ecology, 88, 1379–1385, 2007.

Schmidt, S. K., Wilson, K. L., Monson, R. K., and Lipson, D. A.: Exponential growth of "snow molds" at sub-zero temperatures: an explanation fro high beneath-snow respiration rates and Q_{10} values, Biogeochemistry, 95, 13–21, 2009.

Sommerfeld, R. A., Mosier, A. R., and Musselman, R. C.: CO_2, CH_4 and N_2O flux through a Wyoming snowpack and implications for global budgets, Nature, 361, 140–142, 1993.

Stone, R. S., Dutton, E. G., Harris, J. M., and Longenecker, D.: Earlier spring snowmelt in northern Alaska as an indicator of climate change, J. Geophys. Res., 107, ACL 10-1–ACL 10-13, doi:10.1029/2000JD000286, 2002.

Sturm, M., Racine, C., and Tape, K.: Climate change: Increasing shrub abundance in the Arctic, Nature, 411, 546–547, doi:10.1038/35079180, 2001.

Sturm, M., Schimel, J., Michaelson, G., Welker, J. M., Oberbauer, S. F., Liston, G. E., Fahnestock, J., and Romanovsky, V.: Winter biological processes could help convert Arctic tundra to shrubland, BioScience, 55, 17–26, 2005.

Suzuki, R., Kim, Y., and Ishii, R.: Sensitvity of the back scatter intensity of ALSO/PALSAR to the above-ground biomass and other biophysical parameters of boreal forest in Alaska, Polar Science, 7, 100–112, 2013.

Tarnocai, C., Canadell, J. G., Schuur, E. A. G., Kuhry, P., Mazhitova, G., and Zimov, S.: Soil organic carbon pools in the northern circumpolar permafrost region, Global Biogeochem. Cy., 23, GB2023, doi:10.1029/2008GB003327, 2009.

Tojo, M. and Newsham, K. K.: Snow moulds in polar environments, Fungal Ecol., 5, 395–402, 2012.

Timling, I. and Taylor, D. L.: Peeking through a frosty window: molecular insights into the ecology of Arctic soil fungi, Fungal Ecol., 5, 419—429, 2012.

Verbyla, D.: The greening and browning of Alaska based on 1982–2003 satellite data, Global Ecol. Biogeogr., 17, 547–555, 2008.

Whalen, S. C. and Reeburgh, W. S.: A methane flux time series for tundra environments, Global Biogeochem. Cy., 5, 261–273, 1988.

Winston, G. C., Stephens, B. B., Sundquist, E. T., Hardy, J. P., and Davis, R. E.: Seasonal variablility in CO_2 transport through snow in a boreal forest, in: Biogeochemistry of Seasonally Snow-Covered Catchments, edited by: Tonnessen, K. A., Williams, M. W., and Tranier, M., IAHS Publ., 228, 61–70, 1995.

Winston, G. C., Sundquist, E. T., Stephens, B. B., and Trumbore, S. E.: Winter CO_2 fluxes in a boreal forest, J. Geophys. Res., 102, 28795–28804, 1997.

Xu, M. and Qi, Y.: Soil-surface CO_2 efflux and its spatial and temporal variations in a young ponderosa pine plantation in northern California, Glob. Change Biol., 7, 667–677, 2001.